The Astrophysical Journal Letters, 978:L33 (5pp), 2025 January 10 https://doi.org/10.3847/2041-8213/ada37f


# Newest Measurements of Hubble Constant from DESI 2024 Baryon Acoustic Oscillation Observations

Wuzheng Guo[1,2], Qiumin Wang[1,2], Shuo Cao[1,2], Marek Biesiada[3], Tonghua Liu[4], Yujie Lian[1,2], Xinyue Jiang[1,2], Chengsheng Mu[1,2], and Dadian Cheng[1,2]
[1] Institute for Frontiers in Astronomy and Astrophysics, Beijing Normal University, Beijing 102206, Peoples Republic of China; caoshuo@bnu.edu.cn
[2] School of Physics and Astronomy, Beijing Normal University, Beijing 100875, People's Republic of China
[3] National Centre for Nuclear Research, Pasteura 7, PL-02-093 Warsaw, Poland; Marek.Biesiada@ncbj.gov.pl
[4] School of Physics and Optoelectronic, Yangtze University, Jingzhou 434023, People's Republic of China; liutongh@yangtzeu.edu.cn
*Received 2024 November 09; revised 2024 December 18; accepted 2024 December 26; published 2025 January 8*

## Abstract

In this Letter, we use the latest results from the Dark Energy Spectroscopic Instrument (DESI) survey to measure the Hubble constant. Baryon acoustic oscillation (BAO) observations released by the DESI survey, allow us to determine $H_0$ from the first principles. Our method is purely data-driven and relies on unanchored luminosity distances reconstructed from Type Ia supernovae (SN Ia) data and $H(z)$ reconstruction from cosmic chronometers. Thus, it circumvents calibrations related to the value of the sound horizon size at the baryon drag epoch or intrinsic luminosity of SN Ia. We find $H_0 = 68.4^{+1.0}_{-0.8}$ km s$^{-1}$ Mpc$^{-1}$ at a 68% confidence level, which provides the Hubble constant at an accuracy of 1.3% with minimal assumptions. Our assessments of this fundamental cosmological quantity using the BAO data spanning the redshift range $z = 0.51$–$2.33$ agree very well with Planck's results and TRGB results within $1\sigma$. This result is still in a $4.3\sigma$ tension with the results of the Supernova H0 for the Equation of State.

*Unified Astronomy Thesaurus concepts:* Hubble constant (758); Cosmological parameters (339); Observational cosmology (1146)

## 1. Introduction

As one of the most fundamental cosmological parameters, the Hubble constant ($H_0$) plays an important role in understanding our Universe, especially its current expansion rate, composition, and ultimate fate. However, the $H_0$ values deduced from observations of the early and late Universe do not agree with each other. In the last decade, this so-called "Hubble tension" has become an intriguing problem in modern cosmology. Type Ia supernovae (SN Ia) and cosmic microwave background (CMB) radiation are two well-established cosmological probes. The SN Ia based measurement follows from the astronomical distance ladder in the local Universe, while CMB, which froze the temperature fluctuation after the Big Bang, infers $H_0$ value from the inverse distance ladder based on a cosmological model; ΛCDM being the assumed standard model. Specifically, the Supernova H0 for the Equation of State (SH0ES) project favored a higher value of $H_0 = 73.04 \pm 1.04$ km s$^{-1}$ Mpc$^{-1}$ (D. Brout et al. 2022), while the Planck collaboration (CMB measurements) provided a different lower value of $H_0 = 67.4 \pm 0.5$ km s$^{-1}$ Mpc$^{-1}$ (Planck Collaboration et al. 2020). Currently, the Hubble tension has reached a significance level of $5\sigma$–$6\sigma$, making it difficult to explain as a mere statistical fluke. Accordingly, there is intense work in the literature discussing whether our current standard cosmological model (ΛCDM) needs to be replaced with the new physics, e.g., interacting dark energy models (G. R. Farrar & P. J. E. Peebles 2004; E. Di Valentino et al. 2017; W. Yang et al. 2018), f(T) theories (A. A. Starobinsky 2007; G. R. Bengochea 2011), etc. In order to alleviate the $H_0$ tension, great efforts have also been made to identify and overcome systematic effects that can affect the astrophysical distance measurements (M. Rigault et al. 2015; D. N. Spergel et al. 2015; S. Vagnozzi 2020; T. Liu et al. 2023b; Chen et al. 2024). In this respect, the emergence of completely new cosmological-model-independent methods for inferring the value of $H_0$ is very important. For instance, J. L. Bernal et al. (2016) reconstructed the late time expansion history and extrapolated toward $H_0$ using baryon acoustic oscillations (BAO) and SN Ia data. It should be mentioned that their reconstructions rely on the sound horizon scale $r_d$ at the radiation drag epoch, which would be an extra parameter brought into the analysis. Recently, F. Renzi & A. Silvestri (2023) proposed a new methodology to constrain $H_0$ only based on the distance duality relation (DDR hereafter) and direct standard observations, i.e., SN Ia, BAO, and cosmic chronometers (CC) data. In this Letter, inspired by the latest Dark Energy Spectroscopic Instrument (DESI) survey data release, we follow their work and update the constraints on the Hubble constant at different redshifts, trying to find new clues to fix the Hubble tension.

Around the recombination epoch of our Universe, when the photons decoupled from baryonic particles, the features of matter clustering were imprinted on the matter distribution and stretched with the expansion of the Universe. Nowadays, we can observe these features by measuring the galaxy correlation functions and finding a single localized peak in it. The scale corresponding to the peak position is the comoving galaxy separation of $r_d \sim 150$ Mpc, which makes BAO a standard ruler in cosmic research. Apparently, the measurement of the accurate value of this scale relied on a large field sky survey project, so Sloan Digital Sky Survey (SDSS) gave us the first BAO feature measurement in 2005 (D. J. Eisenstein et al. 2005). A few years later, a sample containing 11 data from

BAO observations was established (F. Beutler et al. 2011; A. Font-Ribera et al. 2014; A. J. Ross et al. 2015; S. Alam et al. 2017; J. E. Bautista et al. 2017; M. Ata et al. 2018; J. Ryan et al. 2019). This sample initiated great progress in constraining cosmological models (Y. Lian et al. 2021; W. Guo et al. 2022). However, not all the data in that sample could be used in our research since some of their measurements could not get rid of the effect of $r_{\rm d}$, which would introduce unnecessary priors.

As a successor of the previous SDSS survey, Data Release 1 (DR1) from the new DESI survey, which aimed at scanning over 14,200 squared degrees in the redshift range $0.1 < z < 4.2$ for 5 yr of observations, has produced exciting results from BAO measurements. A recent DESI data release provided five new BAO measurements with transverse comoving distance $D_{\rm M}$ and comoving distance along the line of sight $D_{\rm H}$, which made it possible to eliminate $r_{\rm d}$ (DESI Collaboration et al. 2024a, 2024b, 2024c). We use this opportunity in our constraints since $r_{\rm d}$ derived from CMB observations would bias our results. The DESI data relevant to our work was measured from luminous red galaxies (LRG), emission-line galaxies (ELG) as direct tracers, and indirect Lyman-$\alpha$ (Ly$\alpha$) forest quasars tracing through the distribution of neutral hydrogen. Combined with the other two tracers from the low redshift galaxies of bright galaxy sample (BGS) and QSO, which we did not use in our analyses, DESI Collaboration et al. (2024a) required $H_0 = 68.52 \pm 0.62\ {\rm km\ s^{-1}\ Mpc^{-1}}$ with priors from Big Bang nucleosynthesis and CMB. This new data release also promoted testing new ideas for relieving the Hubble tension (T. Clifton & N. Hyatt 2024).

## 2. Method

The Hubble constant is directly linked to the distances measured from extragalactic objects within our Universe. More precisely, these distances can be further categorized into luminosity distance $d_{\rm L}$ and angular diameter distance $d_{\rm A}$. The former is derived from the observed emission flux of a source of known intrinsic luminosity, while the latter is based on knowledge of the intrinsic angular size of the object. These two types of distances are linked together through the DDR, which is expressed as

$$\frac{d_{\rm L}(z)}{(1+z)^2 d_{\rm A}(z)} = 1. \tag{1}$$

Such relation is valid in any metric theory of gravity and requires two conditions needed to be met: that photons propagate along null geodesics, and their number is conserved during the propagation. Various tests have been done so far to verify the validity of the DDR by testing the above ratio (S. Cao & N. Liang 2011; S. Cao et al. 2016; J.-Z. Qi et al. 2019; X. Zheng et al. 2020; T. Liu et al. 2023a) consistently justified the validity of Equation (1).

Now the Hubble constant can be formulated as

$$H_0 = \frac{1}{(1+z)^2}\frac{\Xi_{\rm SNIa}(z)}{\Xi_{\rm BAO}(z)} H_{\rm CC}(z), \tag{2}$$

which expresses $H_0$ in terms of independently observable quantities. On the one hand, $\Xi_{\rm SNIa}(z) = H_0 d_{\rm L}(z)$ is the unanchored luminosity distance, associated with SN Ia observations through their measurements of apparent magnitude. On the other hand, $\Xi_{\rm BAO}(z) = H(z) d_{\rm A}(z)$ is the product of the Hubble parameter ($H(z)$) and the angular diameter distance ($d_{\rm A}(z)$). Especially, this product can be calculated by combining the transverse and line-of-sight comoving distances from BAO measurements, without relying on the value of sound horizon $r_{\rm d}$ at the drag epoch. The CCs offer a direct measurement of the Hubble parameter $H(z)$ by using the differential ages of galaxies, which are determined by the evolution of passively aging star populations and their spectroscopic redshifts.

Five data points regarding BAO measured by DESI are central to our implementation of Equation (2). Therefore, the other data sets, i.e., standard clocks (CC), and standard candles (SN Ia) should provide the necessary ingredients at the redshifts corresponding to the BAO measurements. Simple interpolation would introduce too much uncertainty and bias to the final results. Therefore, in our Letter, we use the Gaussian processes (GP) regression to reconstruct SN Ia and CC data at BAO's redshifts. This approach is different from traditional GP by assuming that observational data adhere to N-dimensional Gaussian distributions centered around an input prior mean function (K. Liao et al. 2019; 2020; X. Li et al. 2024; T. Liu & K. Liao 2024; T. Liu et al. 2024). We choose the $\Lambda$CDM model as the mean function in reconstructions (with the fiducial value of matter density parameter $\Omega_{\rm m} = 0.30$). Then, based on the same prior input mean function, different input hyperparameters in GP regression would reconstruct different curves about the required variable, and the best 1000 curves that match the data, whose $\chi^2$ are all smaller than the mean function, are selected as the final reconstruction result in this Letter.

## 3. Data

Our analysis encompasses three publicly accessible data sets: five BAO data points from the DESI Data Release 1 (DESI Collaboration et al. 2024a); the SN Ia sample from the Pantheon+ data set (D. Brout et al. 2022); and a compilation of 32 CC measurements of the Hubble parameter $H(z)$ (J.-Z. Qi et al. 2023).

At the drag epoch of the early Universe, the photons decoupled from the baryons, thus the primary disturbance propagating at the speed of sound was imprinted on the matter distribution. This feature stretched with the expansion of the Universe and appeared as the inhomogeneous distribution of the luminous objects. So, in BAO measurement, this distribution can be measured by counting the number of galaxy pairs at different separation scales and distinguishing the scale related to the peak of the two-point correlation function as the BAO scale at that redshift. Measurable quantities comprise the preferred angular separation of galaxies in the direction perpendicular to the line of sight and preferred redshift separation in the direction along the line of sight. Hence, the ratios $D_{\rm M}/r_{\rm d}$ and $D_{\rm H}/r_{\rm d}$ are observables, and in order to use the distances $D_{\rm M}$ and $D_{\rm H}$ one needs to know the size of the sound horizon $r_{\rm d}$. However, thanks to the DDR, there is no need to use these two distances individually since their ratio can be transformed to $H(z)d_{\rm A}(z)$, which is the same as the denominator of Equation (2),

$$\frac{D_{\rm M}}{D_{\rm H}} = \frac{(1+z)d_{\rm A}(z)}{cH(z)^{-1}} = \frac{1+z}{c} H(z) d_{\rm A}(z), \tag{3}$$

where $c$ is the speed of light.

Up to now, the latest DR1 of DESI only covered half of the expected area of the survey, while it already provided more

than twice the number of redshifts compared with SDSS, achieving a higher precision (about 0.49%) on the BAO isotropic scale (DESI Collaboration et al. 2024a). Due to the possible limitations of the survey time, the signal-to-noise ratio of BGS and QSO tracers was not high enough so only the angle averaged signal was measured. Therefore, only five data points from LRG, ELG, and Ly$\alpha$ tracers are available for our purpose of estimating $H_0$. Due to its high precision, this data set has already been widely used in studying the properties of dark energy (M. Cortês & A. R. Liddle 2024; W. Giarè et al. 2024; H. Wang & Y.-S. Piao 2024), trying to release the Hubble tension (D. Bousis & L. Perivolaropoulos 2024; X. D. Jia et al. 2024), testing modified gravity theory (C. Escamilla-Rivera & R. Sandoval-Orozco 2024).

Regarding SN Ia, the Pantheon+ data set has been significantly expanded in both sample size and redshift coverage compared to its predecessor, the Pantheon data set (D. M. Scolnic et al. 2018). The distance modulus was derived from the Pantheon+SH0ES data set, which included 1701 light-curve measurements from 1550 distinct supernovae spanning a redshift range of $z \in [0.001, 2.26]$. Additionally, the host distance of Cepheid variable stars was determined from 77 data points associated with supernovae in their host galaxies, with a redshift range of $0.00122 < z < 0.01682$. The luminosity distance of SN Ia is related to the distance modulus given by

$$\mu_{\rm SN} \equiv m_{\rm B} - M_{\rm B} = 5\log_{10}\left(\frac{d_{\rm L}}{\rm Mpc}\right) + 25, \tag{4}$$

where $m_{\rm B}$ represents the observed magnitude in the rest-frame B band and $M_{\rm B}$ is the absolute magnitude. Note that $M_{\rm B}$ is tightly correlated with $H_0$. Therefore, following A. G. Riess et al. (2016), we introduce a calibrating term $a_{\rm B} = \log_{10}H_0 - 0.2M_{\rm B} - 5$ instead of the absolute magnitude $M_{\rm B}$ and obtain

$$H_0 d_{\rm L}(z) = 10^{0.2m_{\rm B}+a_{\rm B}}. \tag{5}$$

This unanchored luminosity distance effectively avoids the bias introduced by the degeneracy between $H_0$ and $M_{\rm B}$, and the calibration term was also constrained at $a_{\rm B} = 0.71273 \pm 0.00176$ (A. G. Riess et al. 2016). Hence, we follow this approach in our reconstruction and the uncertainty of $a_{\rm B}$ is included in order to get a robust conclusion. Thus, all the uncertainties in our GP regression reconstruction could be treated using the covariance matrix, which includes both statistical and systematic uncertainties.

For SN Ia, systematic effects can induce correlations among different supernovae, and thus, the optimal fitting point should be adjusted for their presence. Ignoring these effects not only underestimates the uncertainty but may also bias the results (A. Conley et al. 2011). Consequently, we utilize the covariance matrix to marginalize all systematic terms during the fitting process. The reconstructed unanchored luminosity distance ($H_0 d_{\rm L}$) is depicted as blue curves in the left panel of Figure 1, with the dashed black line representing the $\Lambda$CDM model. We also show the reconstruction results with the $w_0w_a$CDM model acting as the mean function (with the dark energy equation of state parameters derived in Z. Wang et al. 2024), since both DESI BAO and Pantheon+ data actually allow for a $w_0w_a$CDM model with $w_0 > -1$ and $w_a < 0$. The reconstructed curves with different mean functions prefer almost the same reconstruction results, which confirms again that the GP regression we use is essentially a model-independent method in the sense that the mean functions only act as a prior in GP regression. Moreover, the reconstruction results with different numbers of lines ($N = 100$, 1000, 2000) are also displayed in Figure 1. Our results suggest that reconstruction curves follow the N-dimensional Gaussian distribution, hence the larger number of curves used for calculating $H_0$ would only help to smooth the posterior distribution and does not improve the resulting mean value of $H_0$ nor its $1\sigma$ range (X. Li et al. 2021; T. Liu & K. Liao 2024). To sum up, using 1000 reconstruction lines with the fiducial $\Lambda$CDM model as the mean function is suitable for the subsequent calculation. For the purpose of calculating $H_0$, we use reconstructed unanchored luminosity distances corresponding to the redshifts of the BAO data points.

The last ingredient we need is the Hubble parameter $H(z)$, which can be expressed as

$$H(z) = -\frac{1}{1+z}\frac{{\rm d}z}{{\rm d}t}, \tag{6}$$

where the redshift $z$ could be obtained from spectroscopic surveys with high accuracy and the differential age evolution of the Universe (d$t$) was derived from the age evolution of massive galaxies. Different from other galaxies, massive ($M_{\rm stars} > 10^{11}M_{\odot}$) early-type galaxies formed >90% of their stellar mass rapidly (at high-redshift $z > 2$–3), and have no subsequent major episode of star formation. Therefore, this type of galaxy provided an ideal environment to measure $H(z)$ due to its age and stable evolution (M. Moresco et al. 2016). This method based on observational $H(z)$ data (OHD) has been widely used to test cosmological models (C. Zhang et al. 2014).

In this Letter, we use the most recent data set, encompassing 32 CCs (J.-Z. Qi et al. 2023), which spans a redshift range from $z = 0.07$ to $z = 1.965$. This approach holds promise for determining the Hubble constant independently of cosmological models, although it is imperative to meticulously assess the associated system uncertainties (M. Moresco et al. 2020). Since there were still some uncertainties in the determination of the physical properties of galaxies, both statical errors and systematic errors were considered in this data set (J.-Z. Qi et al. 2023). The results of our reconstructions, based on this comprehensive sample, are presented in Figure 2. It is evident that our reconstructed data for both SN Ia and CC align well with the predictions of the $\Lambda$CDM model. This concordance reaffirms our approach to adopt the $\Lambda$CDM model as a prior in the GP regression analysis, which could be considered a prudent choice for our study.

## 4. Results and Discussion

Our approach to constrain the Hubble constant from BAO data supplement by SN Ia unanchored distances and CC can be outlined as follows. (I) Reconstruct the unanchored luminosity distance $H_0 d_{\rm L}(z)$ relation and $H(z)$ relation using available compilations of SN Ia data (Pantheon+ sample) and CC, respectively. The GP regression technique is used for this purpose. (II) Our reconstruction contains 1000 $H_0 d_{\rm L}(z)$ and 1000 $H(z)$ curves from which the values corresponding to BAO redshifts are picked. Then, at each BAO redshift, the value of $H(z)d_{\rm A}(z)$ is sampled randomly from the Gaussian distribution representing the measured values and their uncertainties given

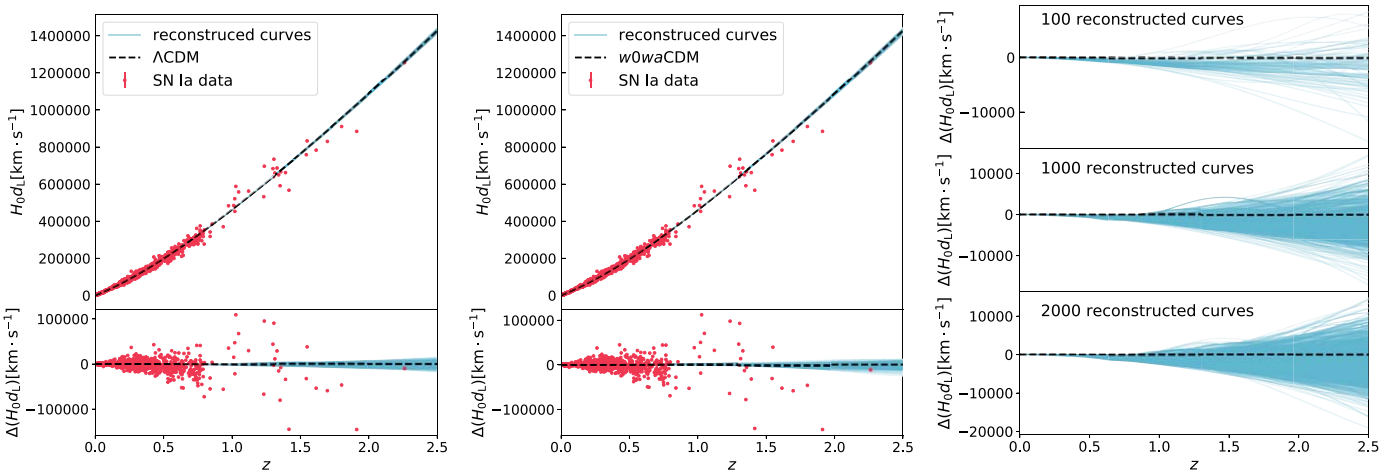


**Figure 1.** Left panel: reconstructed $H_0 d_L$ from SN Ia data using GP regression, with fiducial ΛCDM model as a prior. Middle panel: reconstructed $H_0 d_L$ from SN Ia data using GP regression, with fiducial $w_0 w_a$CDM model as a prior. The residuals between reconstructed $H_0 d_L$ and their input mean functions are also shown in each bottom panel. Right panel: the residuals between reconstructed $H_0 d_L$ and the fiducial ΛCDM with different line numbers. The red dots with the error bar are the SN Ia data set used in reconstruction, the blue curves show our reconstructed results, and the black dashed line presents the mean function in each reconstruction.

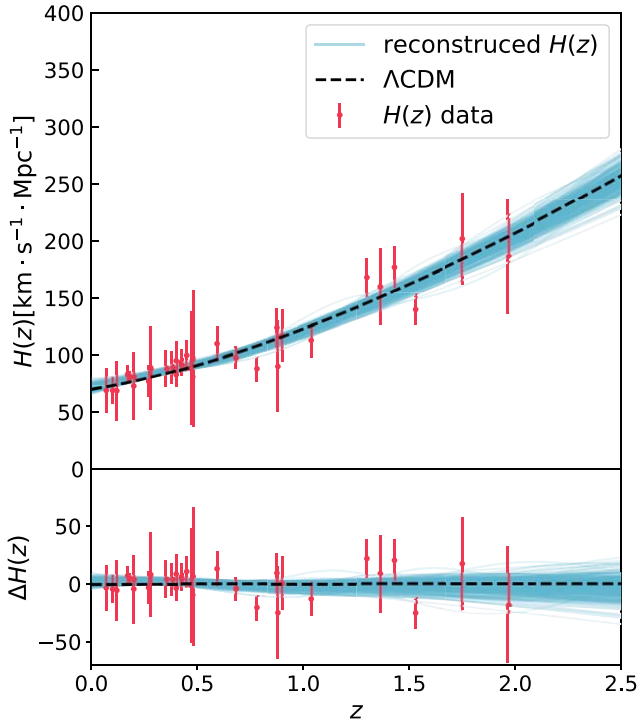


**Figure 2.** Reconstructed $H(z)$ from CC data using GP regression. The black dashed line shows the fiducial ΛCDM model. The residuals between reconstructed $H(z)$ and the fiducial ΛCDM are also shown in the bottom panel.

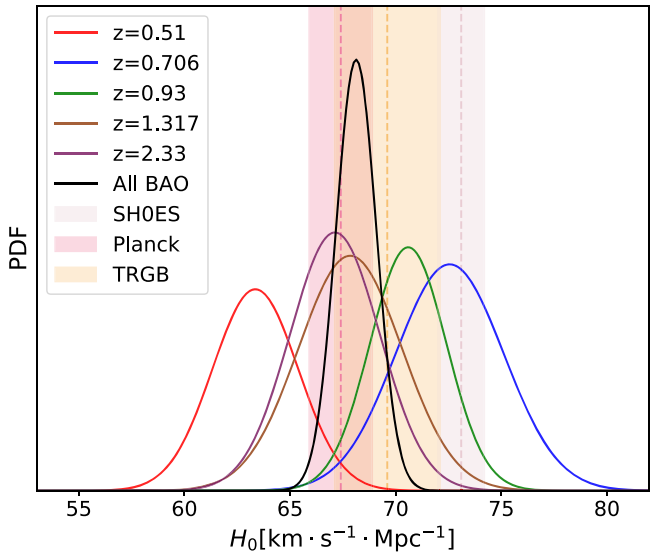


**Figure 3.** Posterior distribution functions (PDFs) of the Hubble constant $H_0$. Shaded regions represent the constraints on $H_0$ and their $1\sigma$ intervals from SH0ES (D. Brout et al. 2022), Planck (Planck Collaboration et al. 2020), and TRGB (W. L. Freedman et al. 2020).

by DESI. This way, 1000 × 1000 possible values for $H_0$ are generated for each redshift. From these values, one-dimensional posterior distribution functions (PDFs) of $H_0$ at five distinct BAO redshifts are derived. (III) Multiply all five PDFs together to establish a comprehensive joint constraint on $H_0$. The advantage of this Letter is that our reconstructions of necessary ingredients are solely data-driven and we do not need to rely on calibrating the absolute magnitude of SN Ia.

Incorporating the most recent data from BAO, we determine the Hubble constant as $H_0 = 68.4^{+1.0}_{-0.8}$ km s$^{-1}$ Mpc$^{-1}$ (median value plus the 16th and 84th percentiles around it). The PDFs of the Hubble constant at five different BAO redshifts

**Table 1**
Value of the Hubble Constant at Different Redshifts Corresponding to BAO Data Points from DESI

| $z$ | $H_0$ (km s$^{-1}$ Mpc$^{-1}$) |
|---|---|
| Total | $68.4^{+1.0}_{-0.8}$ |
| 0.51 | $63.4^{+2.3}_{-2.1}$ |
| 0.706 | $72.4^{+2.8}_{-2.5}$ |
| 0.93 | $70.8 \pm 1.8$ |
| 1.317 | $67.9^{+2.9}_{-2.4}$ |
| 2.33 | $67.5 \pm 2.3$ |

**Note.** The joint posterior $H_0$ value is denoted as total.

and the combined result are depicted in Figure 3, with the numerical constraints detailed in Table 1. Our estimate of $H_0$ is well consistent with the latest results of $H_0 = 68.5 \pm 1.5\,\mathrm{km\,s^{-1}\,Mpc^{-1}}$, based on a combination of independent geometrical data sets (F. Renzi & A. Silvestri 2023). Moreover, the enhanced precision in DESI BAO data has enabled us to achieve a more stringent joint constraint on $H_0$, despite using fewer BAO data points compared with their results. It is noteworthy that the redshift of the Ly$\alpha$ point in BAO data exceeds the redshift ranges of both SN Ia and CC, which would result in some bias when we extend GP regression results. If the Ly$\alpha$ point is not considered in the analysis, the corrected joint estimate is adjusted to $68.6 \pm 1.0\,\mathrm{km\,s^{-1}\,Mpc^{-1}}$, which also agrees with the recent findings obtained under the same assumption (F. Renzi & A. Silvestri 2023). DESI collaboration pointed out that their BAO measurements regarding the LRG tracer showed a $3\sigma$ tension with the SDSS measurements in the redshift range $0.6 < z < 0.8$. The cosmological constraints showed a $2\sigma$ offset in $F_{\mathrm{AP}}$ between the LRG data point in $0.4 < z < 0.6$ and the $\Lambda$CDM expectation (DESI Collaboration et al. 2024a). Therefore, we present here the effect of them on the constraints of the Hubble constant: $H_0 = 69.7^{+1.1}_{-1.0}$ km s$^{-1}$ Mpc$^{-1}$ without LRG1 point, $H_0 = 67.6 \pm 1.0\,\mathrm{km\,s^{-1}\,Mpc^{-1}}$ without LRG2 point, and $H_0 = 69.1^{+1.2}_{-1.1}$ km s$^{-1}$ Mpc$^{-1}$ without LRG1 and LRG2 points. It is clear that the inclusion of the LRG tracer could introduce a nonnegligible influence on the joint result. Especially, in the future analysis of DESI 3 yr and 5 yr data, one should pay more attention to the monopole component in LRG2 (Z. Wang et al. 2024). For the purpose of determining one element necessary for our assessment, i.e., unanchored luminosity distances, we use the Pantheon+ sample of SN Ia. The Pantheon+SH0ES data alone used as cosmological probes (D. Brout et al. 2022) preferred much higher values of $H_0 = 73.4 \pm 1.1\,\mathrm{km\,s^{-1}\,Mpc^{-1}}$, $73.5 \pm 1.1\,\mathrm{km\,s^{-1}\,Mpc^{-1}}$, and $73.3 \pm 1.1\,\mathrm{km\,s^{-1}\,Mpc^{-1}}$ for the $\Lambda$CDM, flat $w$CDM, and flat $w_0w_a$ CDM models, respectively. One might have worried whether this data set could leverage $H_0$ inferred to some higher values. Our findings indicate that on the contrary, our $H_0$ estimate remains consistent with the early Universe's coherent model (Planck Collaboration et al. 2020) and its expansion history (D. J. Eisenstein et al. 2005). Let us remind you that we use BAO alone, without the need to invoke CMB for calibrating the sound horizon scale. Our assessments of this fundamental cosmological quantity, based on the BAO data spanning the redshift range of $z = 0.51$–$2.33$, agree very well with both Planck's results and TRGB results within $1\sigma$ (W. L. Freedman et al. 2020). However, there is still a $4.3\sigma$ tension between our measurements and the results of SH0ES (D. Brout et al. 2022). The redshifts probed by DESI are low as compared with CMB measurements, hence the Hubble tension seems to be not so much about low versus high redshift observations, but the physics of early versus late Universe.

## Acknowledgments

This work is supported by the Beijing Natural Science Foundation No. 1242021; The National Natural Science Foundation of China (Nos. 12021003, 12203009, and 12433001); The Strategic Priority Research Program of the Chinese Academy of Sciences, grant No. XDB23000000; The Interdisciplinary Research Funds of Beijing Normal University, and the Fundamental Research Funds for the Central Universities; The Chutian Scholars Program in Hubei Province (X2023007); and Hubei Province Foreign Expert Project (2023DJC040).

## ORCID iDs

Qiumin Wang https://orcid.org/0009-0003-8646-573X
Shuo Cao https://orcid.org/0000-0002-8870-981X
Marek Biesiada https://orcid.org/0000-0003-1308-7304
Tonghua Liu https://orcid.org/0000-0002-6717-8810
Yujie Lian https://orcid.org/0009-0001-6693-7555

## References

Alam, S., Ata, M., Bailey, S., et al. 2017, MNRAS, 470, 2617
Ata, M., Baumgarten, F., Bautista, J., et al. 2018, MNRAS, 473, 4773
Bautista, J. E., Busca, N. G., Guy, J., et al. 2017, A&A, 603, A12
Bengochea, G. R. 2011, PhLB, 695, 405
Bernal, J. L., Verde, L., & Riess, A. G. 2016, JCAP, 2016, 019
Beutler, F., Blake, C., Colless, M., et al. 2011, MNRAS, 416, 3017
Bousis, D., & Perivolaropoulos, L. 2024, PhRvD., 110, 103546
Brout, D., Scolnic, D., Popovic, B., et al. 2022, ApJ, 938, 110
Cao, S., Biesiada, M., Zheng, X., & Zhu, Z.-H. 2016, MNRAS, 457, 281
Cao, S., & Liang, N. 2011, RAA, 11, 1199
Chen, Y., Kumar, S., Ratra, B., & Xu, T. 2024, ApJL, 964, L4
Clifton, T., & Hyatt, N. 2024, JCAP, 2024, 052
Conley, A., Guy, J., Sullivan, M., et al. 2011, ApJS, 192, 1
Cortês, M., & Liddle, A. R. 2024, JCAP, 2024, 007
DESI Collaboration, Adame, A.G., Aguilar, J., et al. 2024a, arXiv:2404.03002
DESI Collaboration, Adame, A.G., Aguilar, J., et al. 2024b, arXiv:2404.03001
DESI Collaboration, Adame, A.G., Aguilar, J., et al. 2024c, arXiv:2404.03000
Di Valentino, E., Melchiorri, A., & Mena, O. 2017, PhRvD, 96, 043503
Eisenstein, D. J., Zehavi, I., Hogg, D. W., et al. 2005, ApJ, 633, 560
Escamilla-Rivera, C., & Sandoval-Orozco, R. 2024, JHEAp, 42, 217
Farrar, G. R., & Peebles, P. J. E. 2004, ApJ, 604, 1
Font-Ribera, A., Kirkby, D., Busca, N., et al. 2014, JCAP, 2014, 027
Freedman, W. L., Madore, B. F., Hoyt, T., et al. 2020, ApJ, 891, 57
Giarè, W., Sabogal, M. A., Nunes, R. C., & Di Valentino, E. 2024, PhRvL, 133, 251003
Guo, W., Cao, S., Cheng, W., Pan, Y., & Liu, T. 2022, SSPMA, 52, 289510
Jia, X. D., Hu, J. P., & Wang, F. Y. 2024, arXiv:2406.02019
Li, X., Keeley, R. E., Shafieloo, A., & Liao, K. 2024, ApJ, 960, 103
Li, X., Keeley, R. E., Shafieloo, A., et al. 2021, MNRAS, 507, 919
Lian, Y., Cao, S., Biesiada, M., et al. 2021, MNRAS, 505, 2111
Liao, K., Shafieloo, A., Keeley, R. E., & Linder, E. V. 2019, ApJL, 886, L23
Liao, K., Shafieloo, A., Keeley, R. E., & Linder, E. V. 2020, ApJL, 895, L29
Liu, T., Cao, S., Ma, S., et al. 2023a, PhLB, 838, 137687
Liu, T., & Liao, K. 2024, MNRAS, 528, 1354
Liu, T., Yang, X., Zhang, Z., Wang, J., & Biesiada, M. 2023b, PhLB, 845, 138166
Liu, T., Zhong, X., Wang, J., & Biesiada, M. 2024, ApJ, 976, 208
Moresco, M., Jimenez, R., Verde, L., Cimatti, A., & Pozzetti, L. 2020, ApJ, 898, 82
Moresco, M., Pozzetti, L., Cimatti, A., et al. 2016, JCAP, 2016, 014
Planck Collaboration, Aghanim, N., Akrami, Y., et al. 2020, A&A, 641, A6
Qi, J.-Z., Cao, S., Zheng, C., et al. 2019, PhRvD, 99, 063507
Qi, J.-Z., Meng, P., Zhang, J.-F., & Zhang, X. 2023, PhRvD, 108, 063522
Renzi, F., & Silvestri, A. 2023, PhRvD, 107, 023520
Riess, A. G., Macri, L. M., Hoffmann, S. L., et al. 2016, ApJ, 826, 56
Rigault, M., Aldering, G., Kowalski, M., et al. 2015, ApJ, 802, 20
Ross, A. J., Samushia, L., Howlett, C., et al. 2015, MNRAS, 449, 835
Ryan, J., Chen, Y., & Ratra, B. 2019, MNRAS, 488, 3844
Scolnic, D. M., Jones, D. O., Rest, A., et al. 2018, ApJ, 859, 101
Spergel, D. N., Flauger, R., & Hložek, R. 2015, PhRvD, 91, 023518
Starobinsky, A. A. 2007, JETPL, 86, 157
Vagnozzi, S. 2020, PhRvD, 102, 023518
Wang, H., & Piao, Y.-S. 2024, arXiv:2404.18579
Wang, Z., Lin, S., Ding, Z., & Hu, B. 2024, MNRAS, 534, 3869
Yang, W., Pan, S., Di Valentino, E., et al. 2018, JCAP, 2018, 019
Zhang, C., Zhang, H., Yuan, S., et al. 2014, RAA, 14, 1221
Zheng, X., Liao, K., Biesiada, M., et al. 2020, ApJ, 892, 103